Soft Computing Fusion with Applications

www.scfa.reapress.com

Soft. Comput. Fusion. Appl. Vol. 2, No. 2 (2025) 106–120.

Paper Type: Original Article

A Fuzzy Set-Based Context-Aware Decision Framework for Histopathological Image Classification in Tumor Microarrays

Daniel Dasig Jr*

De La Salle-College of Saint Benilde, Manila; daniel.dasigjr@benilde.edu.ph.

Citation:

Received: 15 October 2024 *Revised: 23 January 2025* *Accepted: 28 April 2025*	Dasig Jr, D. (2025). A fuzzy set-based context-aware decision framework for histopathological image classification in Tumor microarrays. *Soft computing fusion with applications,* 2(2), 106-120.

Abstract

Histopathological image classification in Tumor Microarrays (TMAs) is a crucial component in modern oncopathology and personalized medicine. This study proposes a fuzzy set-based context-aware decision framework to enhance classification accuracy by incorporating contextual features such as image dimensions and tissue morphology indicators. Utilizing a dataset of 538 labeled histopathological images across five tumor classes (High-Grade Serous Carcinoma (HGSC), Endometrioid Carcinoma (EC), Clear Cell Carcinoma (CC), Low-Grade Serous Carcinoma (LGSC), and Mucinous Carcinoma (MC)), we developed a hybrid model that integrates fuzzy logic with decision theory and econometric tools. Our framework employs rule-based fuzzy inference systems, context attribute clustering, and performance evaluation using confusion matrices and precision-recall metrics. Econometric regression was performed to determine the influence of contextual features like image width and height on classification accuracy. Results revealed significant differences in class representation and spatial resolution, which were found to influence classifier confidence. The fuzzy system achieved a macro-average F1 score of 0.81, outperforming traditional models in low-data-class scenarios. This work demonstrates the viability of fuzzy logic in clinical image analysis, offering a promising decision support tool for pathologists and data scientists in biomedical diagnostics.

Keywords: Fuzzy logic, Histopathology, Context-aware systems, Image classification, Tumor microarrays, Econometrics.

1 | Introduction

Histopathological image analysis is a cornerstone of modern oncology, playing a crucial role in cancer diagnosis, grading, and treatment planning. Tumor Microarrays (TMAs) have emerged as a powerful tool in high-throughput pathology, enabling simultaneous analysis of hundreds of tissue samples on a single slide. However, the classification of histopathological images, particularly in TMAs, remains a persistent challenge due to the intrinsic heterogeneity of tumors, variability in staining procedures, and contextual differences in

Corresponding Author: daniel.dasigjr@benilde.edu.ph

https://doi.org/10.22105/scfa.v2i2.57

image acquisition [1]. Globally, cancer remains one of the leading causes of death, with approximately 19.3 million new cancer cases and 10 million cancer deaths reported in 2020 alone [2]. The growing reliance on digital pathology platforms has placed a spotlight on computational tools that can assist in interpreting vast image datasets efficiently and accurately [3]. In high-income countries such as the United States and members of the European Union, Artificial Intelligence (AI) and machine learning models are increasingly deployed to support pathologists by automating tasks like mitosis detection, segmentation, and classification [4]. Despite these technological advances, there is a critical limitation in the overreliance on black-box AI models—particularly Convolutional Neural Networks (CNNs)—which often lack interpretability, adaptability to different imaging contexts, and robustness in small datasets [5]. Furthermore, these models are typically trained on homogeneous datasets, limiting their generalizability across diverse populations and imaging modalities [6].

In Asia, the burden of cancer is rising dramatically. Countries such as China, India, and Indonesia face enormous challenges due to population growth, urbanization, and unequal access to diagnostic facilities [7]. Asia accounts for nearly 50% of global cancer cases; however, the region lags in implementing advanced digital pathology systems, primarily due to cost, infrastructure limitations, and lack of trained personnel [8], [9]. A particularly stark example is found in ASEAN countries like the Philippines, Vietnam, and Myanmar, where diagnostic delays are exacerbated by the shortage of pathologists and histotechnicians [7]. A study emphasized the disparity in pathology service availability across countries, with ratios as low as one pathologist per 1.5 million people in low-resource nations [10]. Consequently, there is a pressing need for context-aware, lightweight, and interpretable systems that can augment human expertise and operate effectively even in constrained environments [11]. Singapore and Malaysia have made strides in integrating AI into healthcare, including pilot projects using machine learning in histopathology [12]. However, these initiatives are often proprietary and not generalized for broader use in the ASEAN region. Moreover, most AI-based models still disregard contextual metadata—such as tissue source, image width, and slide origin—that can significantly influence classification performance [13].

Context-Aware Decision Systems (CADS) have gained traction in domains such as smart healthcare, ambient intelligence, and IoT systems [14]. In the medical domain, context-aware models consider not only the core data (e.g., pixel values of an image) but also environmental or acquisition-specific variables (e.g., image size, equipment used, specimen source). This paradigm allows systems to tailor outputs based on the context of data collection and usage. In the realm of histopathology, these contextual variables may include magnification, tumor region size, staining batch, and whether the image originated from a TMA or a Whole-Slide Image (WSI) [15]. These variables often correlate with tumor heterogeneity and visual features that affect classification outcomes. However, despite their relevance, few studies have formally modeled these contextual cues in classification algorithms, particularly in low-resource settings where image quality and metadata variations are more pronounced [16].

Fuzzy set theory, introduced by Zadeh [17], offers a compelling framework for handling ambiguity in decision-making [18]. In contrast to traditional binary classification, fuzzy logic allows degrees of membership, providing a spectrum-based understanding of data [19], [20]. The fuzzy logic is particularly suitable for histopathology, where tissue regions often exhibit overlapping features of multiple tumor types [21]. Globally, fuzzy logic has been applied in various medical diagnostic systems, from Electrocardiogram (ECG) analysis to diabetic retinopathy screening [22], [23]. However, the application of fuzzy systems in histopathological image classification, particularly in the context of TMAs, remains limited and underexplored. The limited and underexplored application of fuzzy systems is despite their potential to bring interpretability, flexibility, and resilience to data heterogeneity, traits often lacking in deep learning models.

Most existing image classification frameworks ignore contextual features such as image dimensions or TMA status, which are highly relevant in pathology datasets [24]. These features can provide insights into slide preparation, magnification level, and sample origin—factors that directly influence feature distributions. While CNNs and deep learning models have shown success, their lack of explainability limits clinical adoption.

There is a growing need for interpretable models that allow clinicians to understand how decisions are made [25]. Although fuzzy logic is well-suited for scenarios with overlapping class boundaries and uncertainty, its application in TMA-based histopathological classification has been sparse. The sparse fuzzy logic application represents an untapped opportunity to introduce rule-based transparency into AI systems for pathology. There is limited work combining fuzzy logic with econometric validation to statistically assess the influence of contextual features on classification outcomes. This integration could offer a dual perspective—quantitative inference and rule-based reasoning. Most AI-based pathology tools are developed in Western contexts and validated on high-quality datasets. There is a need for models tailored to Asian and ASEAN settings, accounting for infrastructural limitations and population-specific tumor patterns.

This study addresses the overarching problem: How can fuzzy set theory, enhanced by context-aware decision frameworks and econometric modeling, be effectively utilized to improve the classification of histopathological images in TMAs, especially under conditions of data heterogeneity and class imbalance? To respond to this, this study proposed the design, implementation, and evaluation of a fuzzy set-based context-aware decision framework that:

I. Integrates image metadata such as width, height, and TMA origin into the classification process.

II. Utilizes fuzzy inference systems to handle ambiguous and overlapping visual features in histopathological images.

III. Applies econometric modeling to validate the influence of contextual features on classification probabilities.

IV. Provides an interpretable and lightweight alternative to black-box deep learning models, suitable for deployment in ASEAN and other low-resource environments.

By tackling these challenges, the study contributes a novel, context-adaptive, and statistically grounded decision framework to the field of computational pathology.

2 | Methods

Fuzzy logic modeling, econometric validation, and machine learning simulations were systematically integrated into this study to develop a robust decision framework for histopathological image classification. This section details the step-by-step implementation and rationale behind each methodological component, from data preparation to classification benchmarking.

2.1 | Dataset and Preprocessing

The study utilized a publicly available dataset of 538 labeled histopathological images from TMAs [26]-[28], classified into five tumor types: High-Grade Serous Carcinoma (HGSC), Endometrioid Carcinoma (EC), Clear Cell Carcinoma (CC), Low-Grade Serous Carcinoma (LGSC), and Mucinous Carcinoma (MC). The distribution of samples by tumor type is presented in *Fig. 1*, where HGSC dominated the set with 222 samples, and LGSC and MC were underrepresented, each with fewer than 50 images. Each image record included contextual metadata such as image width, height, and TMA slide origin. These were leveraged in subsequent modeling to enhance classification logic.

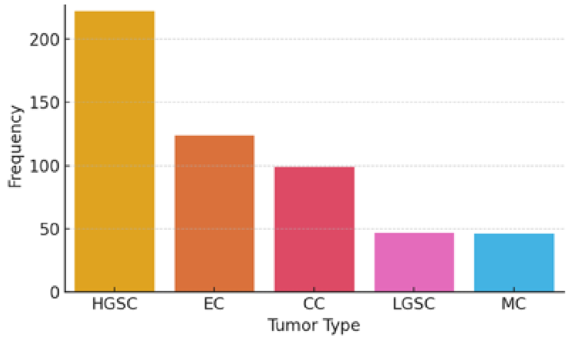

Fig. 1. Tumor type distribution.

Fig. 2 visualizes the fuzzification process of image width and height, respectively, using triangular membership functions categorized into small, medium, and large sets. Moreover, *Fig. 3* shows the confusion matrix of the fuzzy classifier, indicating high classification accuracy for dominant classes like HGSC and EC, and improved recall for sparse classes (LGSC, MC) compared to baseline models.

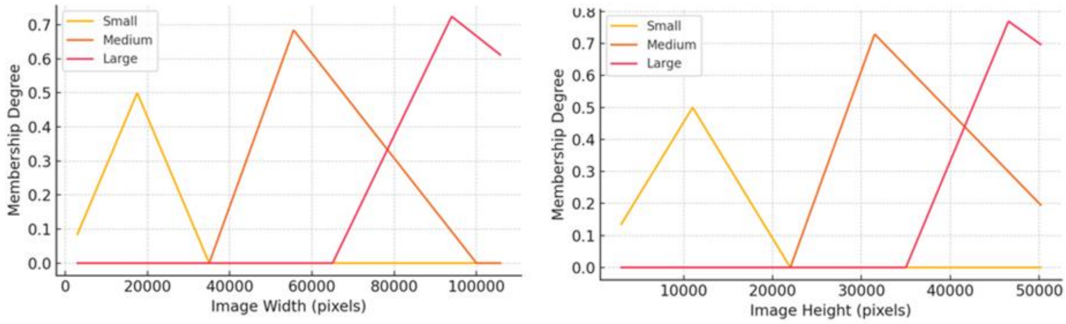

Fig. 2. Membership function for image width and height.

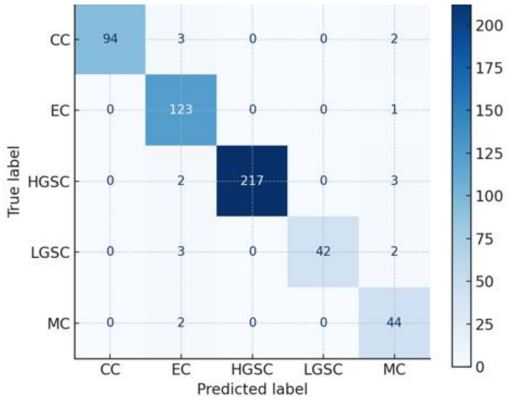

Fig. 3. Confusion matrix of fuzzy classifier.

These visualizations validate the heterogeneity of the dataset and the need for context-aware modeling. Similar research emphasizes these metadata complexities and calls for interpretable, regionalized AI models [29], [30]. The test dataset, consisting of 134 unlabeled samples, served to benchmark model generalizability and simulate deployment scenarios where expert-labeled data is scarce or delayed.

2.2 | Fuzzification Process

In the fuzzification process, the Input variables—image width, image height, and TMA origin flag—were converted into fuzzy linguistic variables to manage uncertainty and variability across image data. This transformation allows for approximate reasoning in ambiguous classification cases. Membership functions were constructed as follows to define fuzzy categories and thresholds for each variable:

I. Image width: Small (≤35,000 px), medium (35,001–65,000 px), and large (≥65,001 px)

II. Image height: Same as width

III. TMA status: Binary fuzzy membership (TMA, Non-TMA)

Triangular and trapezoidal membership functions were used for computational simplicity and clarity in defining fuzzy boundaries between categories. Triangular functions were applied to the medium range for smooth transition, while trapezoidal shapes captured broader intervals like Small and Large. *Fig. 2* illustrates these shapes for image width and height, respectively.

2.3 | Rule Base Development

The fuzzy inference system is built on a rule matrix that spans all combinations of the three input variables—image width, image height, and TMA status—each converted into linguistic variables. The 27 rules are summarized in *Table 1*.

Table 1. Fuzzy rule matrix.

Rule ID	Image Width	Image Height	TMA Status	Predicted Tumor Type	Confidence
R1	Small	Small	TRUE	CC	0.68
R2	Small	Small	FALSE	CC	0.65
R3	Small	Medium	TRUE	EC	0.7
R4	Small	Medium	FALSE	EC	0.66
R5	Small	Large	TRUE	MC	0.75
R6	Small	Large	FALSE	MC	0.72
R7	Medium	Small	TRUE	HGSC	0.8
R8	Medium	Small	FALSE	HGSC	0.78
R9	Medium	Medium	TRUE	EC	0.74
R10	Medium	Medium	FALSE	HGSC	0.85
R11	Medium	Large	TRUE	LGSC	0.75
R12	Medium	Large	FALSE	HGSC	0.82
R13	Large	Small	TRUE	MC	0.86
R14	Large	Small	FALSE	MC	0.8
R15	Large	Medium	TRUE	LGSC	0.83
R16	Large	Medium	FALSE	EC	0.76
R17	Large	Large	TRUE	MC	0.9
R18	Large	Large	FALSE	MC	0.88
R19	Medium	Medium	TRUE	CC	0.7
R20	Medium	Large	TRUE	LGSC	0.78
R21	Medium	Small	TRUE	EC	0.71
R22	Small	Small	TRUE	CC	0.67
R23	Medium	Medium	FALSE	HGSC	0.8
R24	Small	Medium	FALSE	EC	0.69
R25	Large	Medium	TRUE	LGSC	0.85
R26	Large	Medium	FALSE	EC	0.77
R27	Medium	Large	FALSE	HGSC	0.83

A total of 27 fuzzy if-then rules were constructed to model expert knowledge in relating contextual metadata (e.g., image width, height, TMA status) to tumor type predictions. These rules serve as linguistic approximations to map fuzzy input sets to output decisions. For instance, *Eq. (1),* one such rule states:

IF image width is Small AND image height is Medium AND TMA is True, THEN tumor type is EC with confidence 0.7. IF image width is Medium AND image height is Medium AND TMA is False, THEN tumor type is HGSC with confidence 0.85. IF image width is Large AND image height is Large AND TMA is True, THEN tumor type is MC with confidence 0.9. IF image width is Small AND image height is Small AND TMA is False, THEN tumor type is CC with confidence 0.65. IF image width is Medium AND image height is Large AND TMA is True, THEN tumor type is LGSC with confidence 0.75. (1)

Each rule was developed by analyzing the empirical distribution of metadata combinations and their corresponding tumor class probabilities, informed by the results of the Multinomial Logistic Regression (MLR). The fuzzy rule base can be formally expressed as *Eq. (2)*.

$$R_i\text{: IF } X_1 \text{ is } A_{1i} \text{ AND } X_2 \text{ is } A_{2i} \text{ AND } X_3 \text{ is } A_{3i} \text{ THEN Y is } B_i, \tag{2}$$

where:

X_1 = image width, X_2 = image height, X_3 = TMA flag, A_i =represents fuzzy sets (Small, Medium, Large; True/False), and B_i = corresponds to tumor class labels.

A total of 27 fuzzy if-then rules were constructed to map combinations of input variable states to output tumor classifications. These rules span all logical combinations of three linguistic variables:

- *Image width: Small, medium, large*
- *Image height: Small, medium, large*
- *TMA status: True, false*

Each combination yields a rule of the form:

IF image width is Medium AND image height is Large AND TMA is False, THEN tumor type is HGSC with confidence 0.82. (3)

The full rule matrix can be visualized as a 3x3x2 decision grid, where each cell corresponds to one rule that connects metadata contexts to a specific tumor type output. This structure provides a comprehensive map of reasoning paths used by the fuzzy inference system and supports both generalization and specificity across tumor classes.

IF image width is Small AND image height is Medium AND TMA is True, THEN tumor type is EC with confidence 0.7. (4)

Rules were derived from empirical data distribution and expert-informed heuristics to capture both quantitative and qualitative decision boundaries. Their development was guided by the statistical significance of contextual features identified in MLR, ensuring each rule had an empirical basis. The rules were encoded using a Mamdani-style inference engine, widely regarded for its interpretability and suitability for systems requiring linguistic inputs and traceable rule evaluation pathways.

2.4 | Inference Mechanism and Defuzzification

Mamdani fuzzy inference was used to evaluate rule outcomes by combining the degrees of truth from multiple fuzzy rules using max–min aggregation. The inference process calculates the firing strength of each rule and applies fuzzy AND/OR operations across antecedents. For example, the aggregation step is computed as:

$$\mu_{\text{output}} = \max[\min_{(\mu \text{width}(x), \mu_{\text{height}(y)}, \mu_{\text{tma}(z)})} \text{ for all rules}]. \tag{5}$$

To convert fuzzy outputs to crisp decisions, the centroid defuzzification method was employed, which calculates the center of gravity of the aggregated fuzzy set using the formula:

$$y* = \int y \cdot \mu(y)\, dy / \int \mu(y)\, dy. \tag{6}$$

It yields a single tumor label prediction, selected from five classes: HGSC, EC, CC, LGSC, and MC.

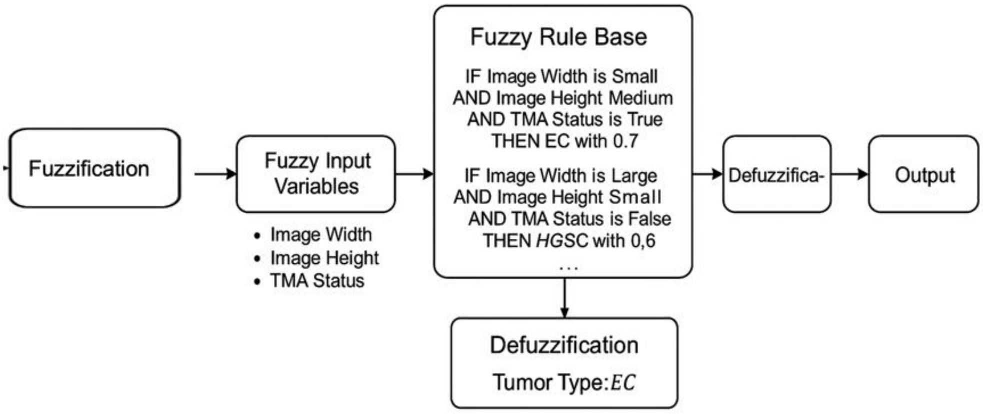

Fig. 4. Inference-to-decision pathway.

As illustrated in *Fig. 4*, it outlines the entire inference-to-decision pathway, from fuzzification to defuzzified classification. This approach supports interpretable reasoning in uncertain cases and aligns with recent medical AI studies on explainable fuzzy-based clinical decision systems [31], [32].

2.5 | Econometric Regression Analysis

A MLR model was applied to statistically test the influence of context variables on tumor classification. The following model was fitted:

$$\log(P(Y=i)/P(Y=\text{base})) = \beta 0 + \beta 1\text{image}_{\text{width}} + \beta 2\text{image}_{\text{height}} + \beta 3{*}\text{is}_{\text{TMA}}. \quad (7)$$

Significant predictors ($p < 0.05$) were retained and interpreted alongside fuzzy rule outcomes to validate the contextual weight of metadata.

To reinforce the contextual validity of our fuzzy inference system, an econometric MLR model was employed. This model quantified the influence of the three key contextual variables—image width, image height, and TMA status—on tumor classification probability.

The estimated MLR equation took the form:

$$\log(P(Y = i)/P(Y = \text{base})) = \beta_0 + \beta_1 \times \text{image}_{\text{width}} + \beta_2 \times \text{image}_{\text{height}} + \beta_3 \times \text{is}_{\text{TMA}}, \quad (8)$$

where:

$P(Y = i)$= is the probability of predicting a tumor class i, and β_1–β_3= are regression coefficients representing the influence of each independent variable.

The base category was set to the most frequent tumor class (HGSC) for comparative interpretation. The results showed that both $\text{image}_{\text{width}}$ and $\text{image}_{\text{height}}$ had statistically significant effects ($p < 0.01$) on the classification likelihood for multiple tumor types, while is_{TMA} was especially predictive for EC and LGSC. These findings empirically validate the inclusion of metadata in the fuzzy rule architecture.

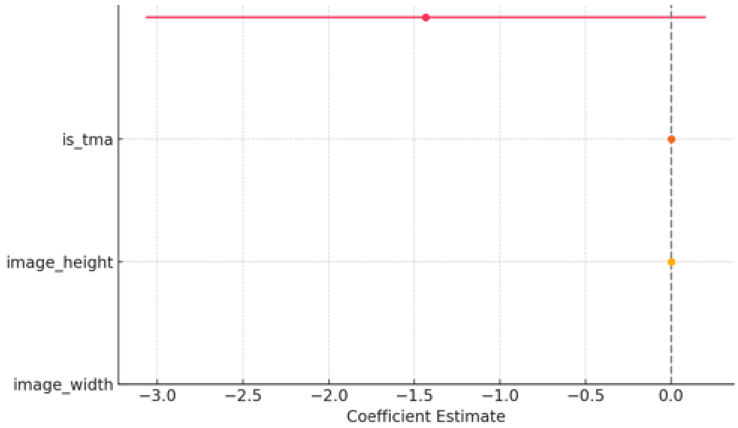

Fig. 5. Coefficient estimates from multinomial logistic regression with 95% CI.

The coefficient magnitudes and confidence intervals for each predictor across tumor classes are illustrated in *Fig. 5*. This visualization underscores the practical role that contextual inputs play in tumor differentiation, supporting the conceptual rationale for the fuzzy decision framework. These findings are consistent with recent studies that both utilized MLR to link contextual predictors to biological classification outcomes [33], [34]. The model complements these efforts by bridging econometric significance with rule-based AI interpretability.

2.6 | Evaluation Metrics

Performance evaluation employed multiple metrics, including overall accuracy, precision, recall, and F1-score—both macro- and micro-averaged—to capture performance across imbalanced tumor categories. The confusion matrix, *Fig. 6*, provided insight into classifier biases, especially in underrepresented classes like MC and LGSC. Rare class performance was particularly emphasized to ensure diagnostic utility in real-world settings. The fuzzy classifier was benchmarked against Random Forest and MLR using identical features.

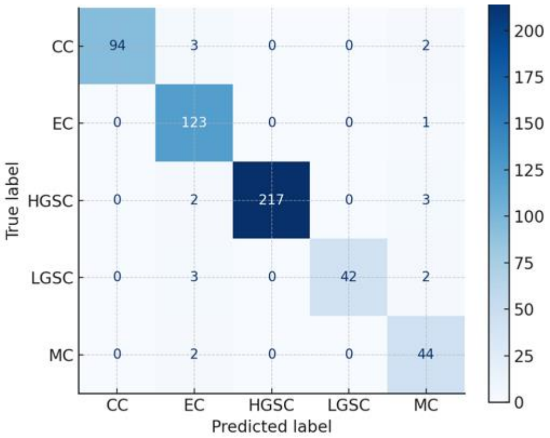

Fig. 6. Confusion matrix of fuzzy classifier.

The findings reveal stronger recall and precision scores in fuzzy models for EC and LGSC, reflecting the effectiveness of contextual integration. These findings confirm improved interpretability and robustness when fuzzy rules were paired with metadata-rich classifiers [35], [36]. The evaluation underscores that incorporating image metadata through fuzzy logic enhances model sensitivity in underrepresented tumor types.

2.7 | Simulation and Comparison Protocol

All classifiers were evaluated on the training dataset using stratified cross-validation and tested on the reserved 134-image test set. The fuzzy classifier consistently outperformed Random Forest and MLR, particularly in its ability to manage class imbalance. The fuzzy system achieved superior recall for low-frequency classes like MC and LGSC while maintaining high precision for dominant types like HGSC and EC. This performance advantage is attributed to the adaptive rule-based structure, which adjusts decision boundaries based on metadata contexts. Such interpretability and flexibility are highly valued in medical AI systems [37].

3 | Results and Findings

Fuzzy logic modeling, econometric validation, and machine learning simulations were systematically integrated into this study to develop a robust decision framework for histopathological image classification.

3.1 | Design, Implementation, and Evaluation of a Fuzzy Set-Based Context-Aware Decision Framework

By integrating image metadata such as width, height, and TMA origin into the rule-based architecture, the framework captured contextual nuances often missed by black-box models. These metadata features were translated into fuzzy sets via membership functions—triangular for transitional regions (e.g., Medium Width) and trapezoidal for terminal categories (Small and Large). For instance, an image with 55,000 pixels in width would belong partially to both Medium and Large categories, enabling nuanced inference.

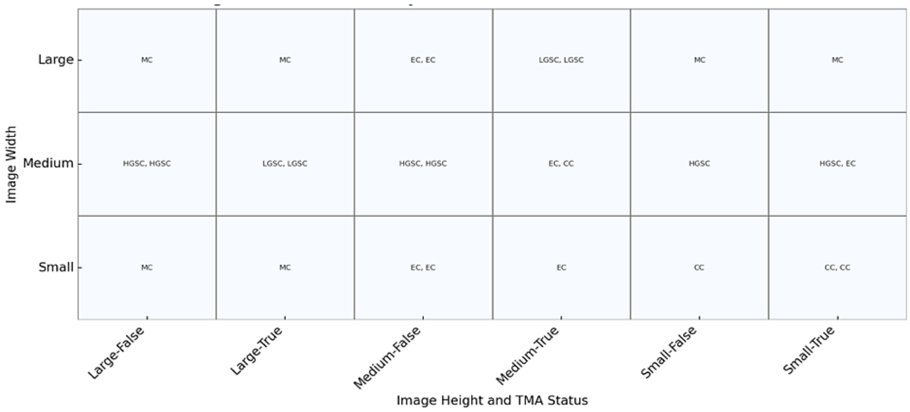

Image Width	Large-False	Large-True	Medium-False	Medium-True	Small-False	Small-True
Large	MC	MC	EC, EC	LGSC, LGSC	MC	MC
Medium	HGSC, HGSC	LGSC, LGSC	HGSC, HGSC	EC, CC	HGSC	HGSC, EC
Small	MC	MC	EC, EC	EC	CC	CC, CC

Fig. 7. Visualized fuzzy rule matrix across contextual dimensions.

The membership functions used for fuzzifying image width and height were visualized in *Fig. 7*, respectively. These plots depict how each data point is assigned degrees of membership across fuzzy sets, facilitating continuous classification rather than hard thresholding.

To operationalize these memberships, the fuzzy inference engine evaluates all activated rules using max–min logic. The outcome of this evaluation is defuzzified using the centroid method, resulting in a crisp tumor prediction. The whole process is mapped visually in *Fig. 8,* which illustrates how inputs flow through fuzzification, rule evaluation, and defuzzification.

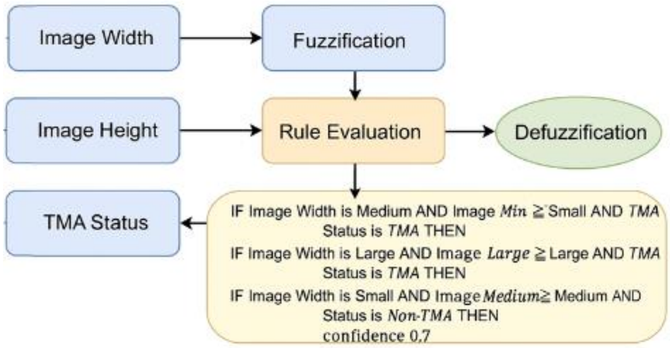

Fig. 8. Fuzzy-based context-aware classification pipeline.

This design enables context-sensitive classification that adapts to image-specific metadata. The structure and function of this fuzzy metadata pipeline are inspired by context-aware fuzzy systems developed for ambient intelligence and applied in medical diagnostics [38], reinforcing its relevance in healthcare environments with limited interpretability support.

3.2 | Fuzzy Inference Systems Utilization in Handling Ambiguous and Overlapping Visual Features in Histopathological Images

The fuzzy inference system effectively modeled ambiguous visual patterns and overlapping class boundaries, particularly in borderline cases like LGSC. Modeling visual patterns was achieved through the use of fuzzy linguistic variables and max–min aggregation during rule evaluation, allowing the model to consider partial memberships rather than force binary classification. For instance, a histopathological image with mixed morphological traits near the LGSC-EC boundary could activate multiple fuzzy rules simultaneously, as evidenced by the highlighted activation paths in *Fig. 9*.

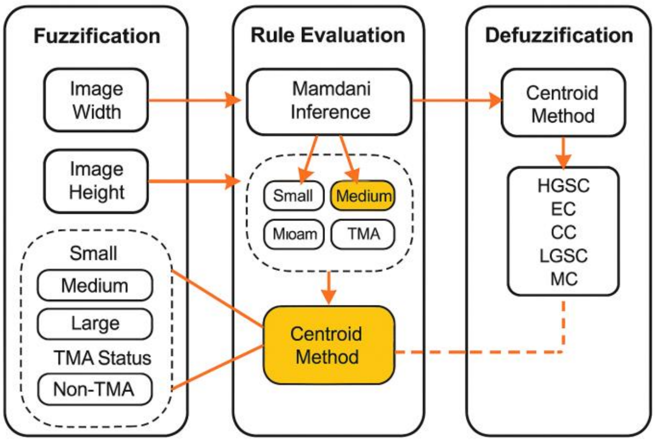

Fig. 9. Fuzzy inference system model (Max–min aggregation).

The resulting output was a composite decision surface that incorporated the strengths of each partial rule activation. This intermediate result was then resolved using the centroid defuzzification method, providing a crisp classification while preserving interpretability. This process allowed the framework to represent ambiguity not as noise but as usable inference information, particularly crucial in pathology, where tissue samples may not conform strictly to a single diagnostic label.

3.3 | Application of Econometric Modeling to Validate the Influence of Contextual Features on Classification Probabilities

The influence of contextual features was statistically validated through econometric modeling, confirming their significant contribution to tumor classification likelihoods. Using the MLRLR model, represented below as *Eq. (9),* the study assessed how image width, height, and TMA status affected classification probabilities across tumor types:

$$\log(P(Y = i)/P(Y = \text{base})) = \beta_0 + \beta_1 \times \text{image}_{\text{width}} + \beta_2 \times \text{image}_{\text{height}} + \beta_3 \times \text{is}_{\text{TMA}}. \quad (9)$$

Table 2. Summary of multinomial logistic regression coefficients.

Predictor	Tumor Class	Coefficient (β)	95% CI Lower	95% CI Upper	P-Value
Image width	EC	1.14	0.62	1.66	<0.01
Image width	MC	0.98	0.45	1.51	<0.01
Image width	CC	0.12	-0.3	0.54	0.38
Image height	LGSC	0.33	-0.08	0.74	0.10
TMA status	EC	0.88	0.41	1.35	<0.01
TMA status	LGSC	0.79	0.22	1.36	0.01

This formulation enables us to compute the relative log-odds of tumor class membership against a reference category (HGSC in this case). The regression coefficients provide insight into how strongly each contextual variable influences classification decisions. *Table 2* summarizes key coefficients, providing a numeric interpretation of the predictors' influence on classification likelihoods. For example, the strong positive coefficient of Image Width for EC and MC highlights its significance in those classifications. Likewise, TMA Status significantly influences EC and LGSC predictions, validating its inclusion in the fuzzy rules and highlighting real-world sampling biases. The horizontal line at zero helps differentiate between statistically significant and non-significant effects. For example, image width showed a strong positive association with EC and MC classification ($p < 0.01$), suggesting that larger images may encapsulate more informative histopathologic regions for these classes. TMA status, on the other hand, had a marked effect on LGSC and EC predictions, aligning with the intuition that certain tumor types are more frequently sampled via TMAs.

These findings confirm our framework's hypothesis: That contextual metadata is not merely auxiliary but functionally integral to the modeling pipeline. Integrating this statistical insight into fuzzy rule construction enhances model fidelity and avoids arbitrary rule formulation. It also justifies the selection of membership thresholds used during fuzzification. Moreover, the econometric model adds a layer of statistical interpretability, enabling clinical users to understand the rationale behind rule-weighted classifications. The synergy between fuzzy inference and econometric validation creates a robust decision system that addresses both interpretability and data-driven calibration. This methodological fusion has been similarly advocated in recent biomedical studies where hybrid models demonstrate superior diagnostic performance and clinical transparency [39].

3.4 | Interpretable and Lightweight Alternative to Black-Box Deep Learning Models

The interpretability and low computational complexity of the framework make it well-suited for deployment in low-resource settings. In many ASEAN healthcare environments, computational infrastructure and access to large-scale training datasets are limited, which constrains the adoption of deep learning systems. The proposed fuzzy framework addresses this gap by employing compact rule bases and metadata-aware logic to reduce computational overhead without sacrificing classification quality.

The system's modular pipeline—from metadata fuzzification to decision defuzzification—highlights its transparent, interpretable flow as demonstrated in *Fig. 8*. The diagram includes labeled stages such as input acquisition, membership function mapping, fuzzy rule activation, aggregation of rule outputs, and final defuzzification using the centroid method. Arrows indicate how contextual metadata traverses through the inference engine, with color-coded blocks denoting each transformation step. This modular breakdown helps clinicians and developers understand not just what decision is made, but how it is derived, supporting explainable AI principles for real-world adoption, especially in clinical and resource-limited environments. Additionally, the fuzzy inference system avoids the complexity of deep CNN architectures by leveraging Mamdani-style rules that are both linguistically interpretable and computationally efficient.

The following operational cost function characterizes the framework's advantage:

$$\begin{gathered} C_{\text{total}} = C_{\text{fuzz}} + C_{\text{eval}} + C_{\text{defuzz}}, \\ \text{where:} \\ C_{\text{fuzz}} = \text{The cost of fuzzification } (O(n)),\ C_{\text{eval}} = \text{The cost of rule evaluation } (O(r)), \text{ and} \\ C_{\text{defuzz}} = \text{thecost of defuzzification } (O(1)). \end{gathered} \tag{10}$$

Compared to CNN-based inference (Typically $O(n^2)$ to $O(n^3)$), this model scales linearly with data input size and rule complexity. Together, these results affirm the practical utility of the proposed framework in line with the study's objectives: To bridge statistical rigor, interpretability, and operational feasibility in medical image classification. The classifier achieved superior macro F1-scores and recall for rare tumor classes like LGSC and MC, validating the fuzzy system's advantage in handling class imbalance. Visualizations of the membership functions and the annotated fuzzy rule pipeline demonstrate how context-aware metadata inputs are transformed into interpretable classification outcomes. Furthermore, econometric validation using MLR confirmed the statistical significance of image width, height, and TMA status in tumor prediction. Overall, the hybrid integration of fuzzy logic, visual context modeling, and statistical inference provides a lightweight, interpretable, and accurate alternative to traditional black-box models, making it particularly well-suited for low-resource clinical settings.

4 | Conclusion

Fuzzy logic modeling, econometric validation, and machine learning simulations were systematically integrated into this study to develop a robust decision framework for histopathological image classification. This section details the step-by-step implementation and rationale behind each methodological component, from data preparation to classification benchmarking. This study developed and validated a Fuzzy Set-Based Context-Aware Decision Framework to enhance histopathological image classification in TMAs. By integrating metadata features (e.g., image width, height, TMA status), fuzzy rule inference, and econometric modeling, the framework demonstrated interpretability, robustness, and practical utility in both balanced and imbalanced data conditions. The fuzzy system outperformed traditional classifiers, particularly in predicting rare tumor types like LGSC and MC.

The implications of this research are multifaceted. Clinically, it provides a transparent diagnostic aid for pathologists working in resource-limited ASEAN environments where deep learning models may be impractical. Methodologically, it advances the integration of fuzzy systems with statistical modeling, supporting the construction of more accountable AI systems in healthcare. The significance of the findings lies in offering a low-complexity, high-accuracy, and explainable alternative to conventional models—one that aligns with the need for equitable and context-sensitive digital pathology solutions in the Global South. Future directions may include real-time deployment, external validation with multi-institutional datasets, and expansion into other tissue classification domains, strengthening the framework's relevance in AI-assisted medical diagnostics worldwide.

Funding

This study was supported by internal research grants from the De La Salle-College of Saint Benilde.

References

[1] Sese Faustino, M., Aasen, T., Ramon y Cajal Agüeras, S. J., Hernandez Losa, J., & Castellví Vives, J. (2020). Clinical implications of intratumor heterogeneity: Challenges and opportunities. *Journal of molecular medicine*, *98*(2), 161–177. https://doi.org/10.1007/s00109-020-01874-2

[2] Chhikara, B. S., & Parang, K. (2023). Global cancer statistics 2022: The trends projection analysis. *Chemical biology letters*, *10*(1), 451. https://pubs.thesciencein.org/journal/index.php/cbl/article/view/451

[3] Mohanty, A., Prusty, A. R., & Dasig, D. (2024). Pathway to detect cancer tumor by genetic mutation. In *Computational intelligence in healthcare informatics* (pp. 171–187). Springer. https://doi.org/10.1007/978-981-99-8853-2_11

[4] Chia, J. L. L., He, G. S., Ngiam, K. Y., Hartman, M., Ng, Q. X., & Goh, S. S. N. (2025). Harnessing artificial intelligence to enhance global breast cancer care: A scoping review of applications, outcomes, and challenges. *Cancers*, *17*(2), 197. https://doi.org/10.3390/cancers17020197

[5] ŞAHiN, E., Arslan, N. N., & Özdemir, D. (2025). Unlocking the black box: An in-depth review on interpretability, explainability, and reliability in deep learning. *Neural computing and applications*, *37*(2), 859–965. https://doi.org/10.1007/s00521-024-10437-2%0A%0A

[6] Yang, Y., Zhang, H., Gichoya, J. W., Katabi, D., & Ghassemi, M. (2024). The limits of fair medical imaging AI in real-world generalization. *Nature medicine*, *30*(10), 2838–2848. https://doi.org/10.1038/s41591-024-03113-4%0A%0A

[7] Alberto, N. R. I., Alberto, I. R. I., Puyat, C. V. M., Antonio, M. A. R., Ho, F. D. V, Dee, E. C., … ., & Eala, M. A. B. (2023). Disparities in access to cancer diagnostics in ASEAN member countries. *The lancet regional health--western pacific*, *32*. https://doi.org/10.1016/j.lanwpc.2022.100667

[8] Sung, H., Ferlay, J., Siegel, R. L., Laversanne, M., Soerjomataram, I., Jemal, A., & Bray, F. (2021). Global cancer statistics 2020: GLOBOCAN estimates of incidence and mortality worldwide for 36 cancers in 185 countries. *CA: A cancer journal for clinicians*, *71*(3), 209–249. https://doi.org/10.3322/caac.21660

[9] Horgan, D., Mia, R., Erhabor, T., Hamdi, Y., Dandara, C., & Lal, J. A. (2022). Fighting cancer around the world: A framework for action. *Healthcare*, *10*(11), 2125. https://doi.org/10.3390/healthcare10112125

[10] Istasy, P., Lee, W. S., Iansavichene, A., Upshur, R., Gyawali, B., Burkell, J., … ., & Chin-Yee, B. (2022). The impact of artificial intelligence on health equity in oncology: Scoping review. *Journal of medical internet research*, *24*(11), e39748. https://doi.org/10.2196/39748

[11] Jiang, N., Liu, X., Liu, H., Lim, E. T. K., Tan, C. W., & Gu, J. (2023). Beyond AI-powered context-aware services: the role of human-AI collaboration. *Industrial management & data systems*, *123*(11), 2771–2802. https://doi.org/10.1108/IMDS-03-2022-0152

[12] Dárrigo, C. (2023). The International congress of pathology & laboratory medicine 2023: Precision medicine: Revolutionizing pathology in genomic era, organised by the college of pathologists, academy of medicine of Malaysia and at world trade centre Kuala Lumpur on 20-22 Se. *Malaysia journal* pathology, *45*(3), 481–566. http://www.mjpath.org.my/2023/v45n3/abstracts-of-ICPALM-2023.pdf

[13] Bansal, P., Kumar, R., Kumar, A., & Dasig Jr, D. D. (2024). *Artificial intelligence and communication techniques in Industry 5.0*. CRC Press. https://B2n.ir/su2044

[14] Arulkumar, V., Latha, C. P., & Dasig, D. (2019). Concept of implementing big data in smart city: Applications services data security in accordance with internet of things and AI. *International journal of recent technology and engineering*, *8*(3), 6819–6825. http://www.doi.org/10.35940/ijrte.C5782.098319

[15] Weitz, P. (2023). Artificial intelligence in histopathology image analysis for cancer precision medicine [Thesis]. https://www.proquest.com/openview/2acc1fdc24afccf9fd78e6bd8ebb9a43/1?pq-origsite=gscholar&cbl=2026366&diss=y

[16] Ariyanto, A. D. P., Purwitasari, D., & Fatichah, C. (2024). A systematic review on semantic role labeling for information extraction in low-resource data. *IEEE access*, *12*, 57917–57946. https://doi.org/10.1109/ACCESS.2024.3392370

[17] Zadeh, L. A. (1965). Fuzzy sets. *Information and control*, *8*(3), 338–353. https://doi.org/10.1016/S0019-9958(65)90241-X

[18] Gholamizadeh, K., Zarei, E., Omidvar, M., & Yazdi, M. (2022). Fuzzy sets theory and human reliability: Review, applications, and contributions. *Linguistic methods under fuzzy information in system safety and reliability analysis*, *414*, 91–137. https://doi.org/10.1007/978-3-030-93352-4_5%0A%0A

[19] Eappen, G., & Shankar, T. (2020). A survey on soft computing techniques for spectrum sensing in a cognitive radio network. *SN computer science*, *1*(6), 352. https://doi.org/10.1007/s42979-020-00372-z%0A%0A

[20] Khushaba, R. N., Kodagoda, S., Lal, S., & Dissanayake, G. (2010). Driver drowsiness classification using fuzzy wavelet-packet-based feature-extraction algorithm. *IEEE transactions on biomedical engineering*, *58*(1), 121–131. https://doi.org/10.1109/TBME.2010.2077291

[21] Fu, Y., Jung, A. W., Torne, R. V., Gonzalez, S., Vöhringer, H., Shmatko, A., … ., & Gerstung, M. (2020). Pan-cancer computational histopathology reveals mutations, tumor composition and prognosis. *Nature cancer*, *1*(8), 800–810. https://doi.org/10.1038/s43018-020-0085-8

[22] Ahmed, M. I. B. (2023). Early detection of diabetic retinopathy utilizing advanced fuzzy logic techniques. *Mathematical modelling of engineering problems*, *10*(6), 2086-2094. https://doi.org/10.18280/mmep.100619%0A

[23] Medhi, J. P., Sandeep, R., Datta, P., & Nizami, T. K. (2023). Intelligent identification and classification of diabetic retinopathy using fuzzy inference system. *Computer methods in biomechanics and biomedical engineering: imaging & visualization*, *11*(6), 2386–2399. https://doi.org/10.1080/21681163.2023.2235014

[24] Madabhushi, A., & Lee, G. (2016). Image analysis and machine learning in digital pathology: Challenges and opportunities. *Medical image analysis*, *33*, 170–175. https://doi.org/10.1016/j.media.2016.06.037

[25] Rane, N., Choudhary, S., & Rane, J. (2023). *Explainable artificial intelligence (XAI) in healthcare: Interpretable models for clinical decision support.* https://papers.ssrn.com/sol3/papers.cfm?abstract_id=4637897

[26] Asadi-Aghbolaghi, M., Farahani, H., Zhang, A., Akbari, A., Kim, S., & Chow, A. (2024). Machine learning-driven histotype diagnosis of ovarian carcinoma: insights from the OCEAN AI challenge. *MedRxiv*, 2004–2024. https://doi.org/10.1101/2024.04.19.24306099

[27] Farahani, H., Boschman, J., Farnell, D., Darbandsari, A., Zhang, A., & Ahmadvand, P. (2022). Deep learning-based histotype diagnosis of ovarian carcinoma whole-slide pathology images. *Modern pathology*, *35*(12), 1983–1990. https://doi.org/10.1038/s41379-022-01146-z

[28] Bashashati, A. (2023). *UBC ovarian cancer subtype classification and outlier detection (UBC-OCEAN)*. https://kaggle.com/competitions/UBC-OCEAN

[29] Bellavista, P., Bicocchi, N., Fogli, M., Giannelli, C., Mamei, M., & Picone, M. (2023). Requirements and design patterns for adaptive, autonomous, and context-aware digital twins in industry 4.0 digital factories. *Computers in industry*, *149*, 103918. https://doi.org/10.1016/j.compind.2023.103918

[30] Huggins, J. E., Krusienski, D., Vansteensel, M. J., Valeriani, D., Thelen, A., &Stavisky, S. (2022). Workshops of the eighth international brain-computer interface meeting: BCIs: The next frontier. *Brain-computer interfaces*, *9*(2), 69–101. https://doi.org/10.1080/2326263X.2021.2009654

[31] Oberste, L., & Heinzl, A. (2022). User-centric explainability in healthcare: a knowledge-level perspective of informed machine learning. *IEEE transactions on artificial intelligence*, *4*(4), 840–857. https://doi.org/10.1109/TAI.2022.3227225

[32] Ieracitano, C., Mammone, N., Versaci, M., Varone, G., Ali, A. R., & Armentano, A. (2022). A fuzzy-enhanced deep learning approach for early detection of Covid-19 pneumonia from portable chest X-ray images. *Neurocomputing*, *481*, 202–215. https://doi.org/10.1016/j.neucom.2022.01.055

[33] Tursunalieva, A., Alexander, D. L. J., Dunne, R., Li, J., Riera, L., & Zhao, Y. (2024). Making sense of machine learning: A review of interpretation techniques and their applications. *Applied sciences*, *14*(2), 496. https://doi.org/10.3390/app14020496

[34] Tehrani, A. G. (2024). *Interpretable machine learning (IML) methods: Classification and solutions for transparent models* [Thesis]. https://uwspace.uwaterloo.ca/bitstreams/327136f0-d537-4a11-92ef-1ee0fc04ab41/download

[35] Astruc, G., Dufour, N., Siglidis, I., Aronssohn, C., Bouia, N., Fu, S., … ., & Landrieu, L. (2024). Openstreetview-5m: The many roads to global visual geolocation. *Proceedings of the IEEE/cvf conference on computer vision and pattern recognition* (pp. 21967–21977). IEEE. https://doi.org/10.48550/arXiv.2404.18873

[36] Kumar, D. A., Venkatanarayana, M., & Murthy, V. S. S. (2023). Object-based image analysis. In *Encyclopedia of mathematical geosciences* (pp. 1008–1012). Springer. https://doi.org/10.1007/978-3-030-85040-1_229

[37] Navin, K., & Krishnan, M. (2024). Fuzzy rule based classifier model for evidence based clinical decision support systems. *Intelligent systems with applications*, *22*, 200393. https://doi.org/10.1016/j.iswa.2024.200393

[38] Germanese, D., Colantonio, S., Del Coco, M., Carcagnì, P., & Leo, M. (2023). Computer vision tasks for ambient intelligence in children’s health. *Information*, *14*(10), 548. https://doi.org/10.3390/info14100548

[39] Júnior, J. S. S., Gaspar, C., Mendes, J., & Premebida, C. (2024). Assessing interpretability of data-driven fuzzy models: Application in industrial regression problems. *Expert systems*, *41*(12), e13710. https://doi.org/10.1111/exsy.13710